SMAR 2019 – Fifth Conference on Smart Monitoring,
Assessment and Rehabilitation of Civil Structures

SMAR 2019

A double-pass method for bridge assessment considering surface roughness using normalized contact point responses

Ying ZHAN [1], Francis T.K. AU [1]

[1] Department of Civil Engineering, The University of Hong Kong, Pokfulam Road, Hong Kong, China

Contact e-mail: yingzhan@connect.hku.hk

ABSTRACT: This paper proposes a method to identify bridge modal parameters and detect possible damage location(s) using an instrumented vehicle based on vehicle-bridge interaction considering surface roughness. Existing vehicle-response-based bridge damage detection methods usually ignore surface roughness as it will contaminate the vehicle response data. The double-pass method is built upon the equations of motion of the bridge and vehicle. Then the normalized contact point response is obtained from the reponses of the vehicle passing on the bridge twice with extra mass added during the second pass. The normalized contact point response is relatively immune to the additional excitations due to surface roughness. The frequencies and mode shapes of the bridge can be further extracted from the normalized contact point acceleration with spectral analysis and Hilbert transform. The damage can be located accordingly using wavelet transform and coordinate modal assurance criterion. The effectiveness of the proposed method is verified by numerical simulation. The result shows that the proposed method can extract bridge frequencies and mode shapes, and identify single and multiple damage scenarios accurately in the presence of surface roughness of different classes.

1 INTRODUCTION

Modal parameter identification and damage detection of bridges have been an active topic in the field of structural health monitoring as many bridges are approaching their designed service lives. In addition, the growing traffic leads to rising demand for convenient non-destructive detection methods. Modal identification and damage detection using the responses of moving test vehicles are one of the promising indirect methods. It is not only convenient because of the less hindrance to traffic, but also economical as it requires fewer sensors on the test vehicle as compared to the many sensors required on a bridge in the direct method. Yang et al (2004) proposed the use of vehicle responses to extract bridge frequencies, and later extended it to construction of bridge mode shapes (Yang et al, 2014). It is also extended to damage location by various researchers, such as Bu et al (2006), Li and Au (2014) and Qi and Au (2017).

One of the impediments to the application of indirect method is the bridge surface roughness, as pointed out by many researchers. The vehicle response is a carrier of the bridge information, which is easily contaminated by noise caused by the bridge surface roughness. Many of the indirect methods suffer from a loss in accuracy even in the presence of a small amount of surface roughness. This paper proposes a method to assess girder bridges in the presence of normal amount of surface roughness. By letting a vehicle run on the bridge twice, with an extra mass added on the vehicle in the second pass, the influence of surface roughness can be greatly eliminated. The normalized contact point acceleration (NCPA) is calculated from the vehicle

acceleration histories of the two passes, which is proved to be relatively immune to surface roughness compared to other quantities such as the vehicle and contact point accelerations. The mode shapes can be estimated from NCPA using Hilbert transform, and any damage can be located using wavelet transform and coordinate modal assurance criterion (COMAC).

2 VIBRATION OF A GIRDER BRIDGE UNDER MOVING VEHICLE

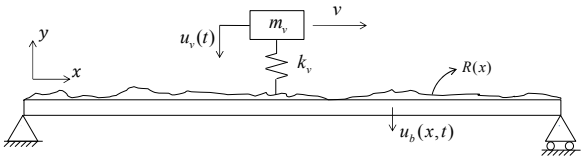

Figure 1. Illustration of the vehicle-bridge interaction system.

Figure 1 shows the vehicle-bridge interaction system of a girder bridge under a moving vehicle, with the governing equations given by

$$\bar{m}\frac{\partial^2 u_b(x,t)}{\partial t^2} + EI\frac{\partial^4 u_b(x,t)}{\partial x^4} = f_c(t)\delta(x-vt) \tag{1}$$

$$m_v\frac{d^2 u_v(t)}{dt^2} + k_v[u_v(t) - u_b(x,t)|_{x=vt} - R(x)|_{x=vt}] = 0 \tag{2}$$

$$f_c(t) = -m_v g + k_v\{u_v(t) - [u_b(x,t)|_{x=vt} + R(x)|_{x=vt}]\} \tag{3}$$

where $\bar{m}$, E, I, $u_b(x,t)$ and $R(x)$ denote the mass per unit length, modulus of elasticity, moment of inertia, vertical displacement and surface roughness of the bridge, respectively; m_v, k_v and $u_v(t)$ are the mass, stiffness and vertical displacement of the vehicle, respectively; t and x denote the location and time, respectively; v is the speed of vehicle; $f_c(t)$ is the contact force between the bridge and vehicle; $\delta(x)$ is the Dirac Delta function; and $\delta(x-vt)$ describes the movement of the contact point. Here the vehicle tire is assumed to be in contact with the bridge surface, which is valid as long as the vehicle speed is not very high (Cheng et al, 1999).

Assuming that the vehicle mass is negligibly small compared to the bridge mass, the displacement of the bridge at the contact point is obtained as

$$u_b(x,t)|_{x=vt} = \sum_{j=1}^{\infty}\frac{-2L^3[m_v g + k_v\tilde{R}(x)]}{j^4\pi^4 EI - j^2\pi^2 v^2 L^2\bar{m}}\sin\frac{j\pi vt}{L}\left[\sin\frac{j\pi vt}{L} - \frac{j\pi v}{L\omega_{bj}}\sin(\omega_{bj}t)\right] \tag{4}$$

where $\omega_{bj} = j^2\pi^2\sqrt{EI/\bar{m}}/L^2$ is the j-th circular frequency of the bridge; and $\tilde{R}(x)$ represents the influence of previous surface roughness on the current bridge response. More details about the derivation process of the Eq. (4) can be found in Zhan and Au (2019). The contact point displacement of the vehicle can be expressed as

$$u_c(t) = [m_v g + k_v\tilde{R}(x)]\bar{u}(t) + R(x)|_{x=vt} \tag{5}$$

where $\bar{u}(t) = \sum_{j=1}^{\infty}\frac{-2L^3}{j^4\pi^4 EI - j^2\pi^2 v^2 L^2\bar{m}}\sin\frac{j\pi vt}{L}\left[\sin\frac{j\pi vt}{L} - \frac{j\pi v}{L\omega_{bj}}\sin(\omega_{bj}t)\right]$ is the normalized bridge contact point displacement, which is the response of the bridge at the contact point under a unit load travelling at the speed v, and is only dependent on the bridge properties such as span length, stiffness and circular frequency while the vehicle properties are not involved except for the vehicle speed v. The normalized bridge contact point displacement $\bar{u}(t)$ cannot be acquired directly from Eq. (5) as $\tilde{R}(x)$ and $R(x)|_{x=vt}$ are unknown. However, if the vehicle passes the bridge twice with different masses m_v and $m_v + m_{add}$, one gets an equation set in terms of

$u_c(t)$ that can be obtained accordingly. Note that $\bar{u}(t)$ is in different form when different vehicle and bridge models are used, but this does not affect the efficacy of the proposed method.

3 BRIDGE ASSESSMENT FROM VIBRATION DATA

3.1 Extraction of bridge frequencies and mode shapes

The normalized bridge contact point displacement $\bar{u}(t)$ is in theory free of the surface roughness contamination, which makes it possible to extract bridge frequency and mode shape from it in the presence of surface roughness. It can be transformed to the following form with trigonometric identities

$$\bar{u}(t) = \sum_{j=1}^{\infty} A_j \left[1 - \cos\frac{2j\pi vt}{L} + \frac{j\pi v}{L\omega_{bj}}\cos\left(\omega_{bj} + \frac{j\pi v}{L}\right)t - \frac{j\pi v}{L\omega_{bj}}\cos\left(\omega_{bj} - \frac{j\pi v}{L}\right)t\right] \quad (6)$$

where $A_j = -2L^3/(j^4\pi^4 EI - j^2\pi^2 v^2 L^2 \bar{m})$. Taking the derivative of $\bar{u}(t)$ twice, NCPA is obtained as

$$\bar{a}(t) = \sum_{j=1}^{\infty} A_j \left[\left(\frac{2j\pi v}{L}\right)^2 \cos\frac{2j\pi vt}{L} - \frac{j\pi v}{L\omega_{bj}}\left(\omega_{bj} + \frac{j\pi v}{L}\right)^2 \cos\left(\omega_{bj} + \frac{j\pi v}{L}\right)t + \frac{j\pi v}{L\omega_{bj}}\left(\omega_{bj} - \frac{j\pi v}{L}\right)^2 \cos\left(\omega_{bj} - \frac{j\pi v}{L}\right)t\right] \quad (7)$$

It is obvious that $\bar{a}(t)$ contains the bridge properties. One can extract the component response corresponding to the bridge frequency of the *j*-th mode from it by a feasible filtering technique. The decomposed bridge component response $a_j(t)$ associated with the *j*-th mode is

$$a_j(t) = A_{rj}\cos\left(\omega_{bj} + \frac{j\pi v}{L}\right)t + A_{lj}\cos\left(\omega_{bj} - \frac{j\pi v}{L}\right)t \quad (8)$$

with $A_{rj} = \frac{L^3}{j^4\pi^4 EI - j^2\pi^2 v^2 L^2 \bar{m}} \frac{j\pi v}{L\omega_{bj}}\left(\omega_{bj} + \frac{j\pi v}{L}\right)^2$, $A_{lj} = -\frac{L^3}{j^4\pi^4 EI - j^2\pi^2 v^2 L^2 \bar{m}} \frac{j\pi v}{L\omega_{bj}}\left(\omega_{bj} - \frac{j\pi v}{L}\right)^2$.

The Hilbert transform is a linear operator that takes a time series $\mu(t)$ and produces its transform pair $\hat{\mu}(t)$, as shown by

$$\hat{\mu}(t) = \frac{1}{\pi t}\,\mathrm{p.v.}\int_{-\infty}^{+\infty}\frac{\mu(\tau)}{t-\tau}d\tau \quad (9)$$

where p.v. denotes the Cauchy principal value. Note that Hilbert transform only applies to narrow band signal and $a_j(t)$ meets such requirement. Therefore, performing the Hilbert transform on $a_j(t)$ gives its transform $\hat{a}_j(t)$ as

$$\hat{a}_j(t) = A_{rj}\sin\left(\omega_{bj} + \frac{j\pi v}{L}\right)t + A_{lj}\sin\left(\omega_{bj} - \frac{j\pi v}{L}\right)t \quad (10)$$

The instantaneous amplitude (or envelope) is defined as the modulus of the transform pairs, i.e.

$$A_j(t) = \sqrt{a_j^2(t) + \hat{a}_j^2(t)} = \sqrt{\left(A_{rj} + A_{lj}\right)^2 - 4A_{rj}A_{lj}\sin^2\frac{j\pi v}{L}t} \quad (11)$$

For the lower modes (e.g. $j \le 3$), $j\pi vt/L$ is much smaller than the bridge frequency ω_{bj}, indicating A_{rj} and A_{lj} are almost identical in magnitude but opposite in sign. Since the lower modes are sufficient for general damage detection purposes, Eq. (11) can be approximated as

$$A_j(t) = \sqrt{-4A_{rj}A_{lj}}\left|\sin\frac{j\pi v}{L}t\right| \quad (12)$$

$A_j(t)$ is the bridge mode shape $\sin(j\pi x/L)$ scaled and in absolute value. Therefore, it is feasible to use the normalized bridge contact point response to get the bridge mode shape.

The double-pass mass-addition technique to extract bridge mode shape is proposed accordingly:

Step 1: Let the vehicle of mass m_v with accelerometer installed on it move on the bridge at a constant speed v and record its vertical acceleration response history $a_1(t)$.

Step 2: Add certain mass on the vehicle so that the total vehicle mass becomes λm_v where λ is a parameter above unity, e.g. 1.5. Let the vehicle with added mass move on the bridge once more at the same speed v and record its vertical acceleration response history $a_2(t)$.

Step 3: Calculate the contact point acceleration histories $a_{c1}(t)$ and $a_{c2}(t)$ and NCPA $\bar{a}(t)$ based on

$$a_{c1}(t) = \omega_v^{-2}\frac{d^2a_1(t)}{dt^2} + a_1(t);\ a_{c2}(t) = \lambda\omega_v^{-2}\frac{d^2a_2(t)}{dt^2} + a_2(t) \tag{13}$$

$$\bar{a}(t) = \frac{a_{c2}(t)-a_{c1}(t)}{(\lambda-1)m_v g} \tag{14}$$

where $\omega_v = \sqrt{k_v/m_v}$ is the vehicle frequency and a_c is the contact point acceleration.

Step 4: Analyze $\bar{a}(t)$ to identify frequency peaks related to bridge frequency using fast Fourier transform or other spectrum analysis tools.

Step 5: Use proper filter to distil the component response $a_j(t)$ that is associated with bridge frequencies from NCPA.

Step 6: Calculate $A_j(t)$, the envelope of $a_j(t)$ with Hilbert transform, adjust the sign of $A_j(t)$ and normalize to get the mode shapes of bridge.

In the field test, the vehicle frequencies can be obtained in advance from measurements of the ambient vibrations. The contact point acceleration can then be obtained from the chassis acceleration using Eq. (13).

3.2 Bridge damage detection using wavelet transform and COMAC

The damage identification is based on the mode shapes obtained previously using wavelet transform and COMAC. Wavelet transform is useful to detect damage as damage deteriorates the completeness of a bridge and leads to singularities on smooth modal parameters such as mode shapes. These irregularities can hardly be observed directly, but wavelet transform serves as a signal microscope and facilitates the detection. The mathematical essence of the wavelet transform is a convolution of the mother wavelet and the signal analyzed, which is expressed as

$$S_w(a,b) = \frac{1}{\sqrt{a}}\int_{-\infty}^{\infty} s(x)\,\bar{\psi}\left(\frac{x-b}{a}\right)dx \tag{15}$$

where $a \in \mathbb{R}^+$ is the scale (elastic) parameter; $b \in \mathbb{R}$ is the translational (shift) parameter; $s(x)$ is the input signal being analyzed; $\psi(x)$ denotes the mother wavelet; and $S_w(a,b)$ represents the wavelet coefficients for scale a and location b. A key issue of using wavelet transform is the selection of proper mother wavelet. This study has adopted the fourth derivative of Gaussian function as mother wavelet, which is expressed as

$$\psi(x) = -\frac{1}{\sqrt{2\pi}}(-3 + 6x^2 - x^4)e^{-\frac{x^2}{2}} \tag{16}$$

COMAC is computed for the mode shapes in intact and damaged conditions for the purpose of damage location. The COMAC value is calculated on each measurement degree-of-freedom by

$$\mathrm{COMAC}_k = \frac{\sum_{j=1}^{m}\left(\varphi_{k,j}^{i}\varphi_{k,j}^{d}\right)^2}{\sum_{j=1}^{m}\left(\varphi_{k,j}^{i}\right)^2\sum_{j=1}^{m}\left(\varphi_{k,j}^{d}\right)^2} \tag{17}$$

where the subscripts k and j denote indices of measurement degree-of-freedom and mode shapes respectively; the superscripts i and d indicate the intact and damaged conditions respectively; and m is the total number of mode shapes used. The condition COMAC = 1 indicates that the bridge is intact.

Note that COMAC requires baseline information while wavelet transform does not. While each damage indicator alone can locate the damage, here the two indicators are adopted together for improved identification.

4 NUMERICAL SIMULATION

The surface roughness is generated according to ISO 8608 (2016) with the lower and upper spatial frequency limits set as 0.1 and 50 m^{-1}, respectively. Five classes of surface roughness from very good (Class A) to very poor (Class E) quality are generated. The vehicle is simulated as a spring-mass with mass m_v = 1000 kg and stiffness k_v = 25000 N/m. 500 kg will be added on the vehicle during the second pass, i.e. λ = 1.5. The simply-supported bridge has a span of 30 m, elastic modulus $E = 3.15\times10^{10}$ N/m^2, mass density ρ = 2500kg/ m^3, second moment of area I = 0.36 m^4 and cross-sectional area A = 1 m^2. The vehicle runs on the bridge at a speed of v = 2 m/s. The simulation is conducted in MATLAB environment and the vehicle-bridge interaction codes are verified with ANSYS.

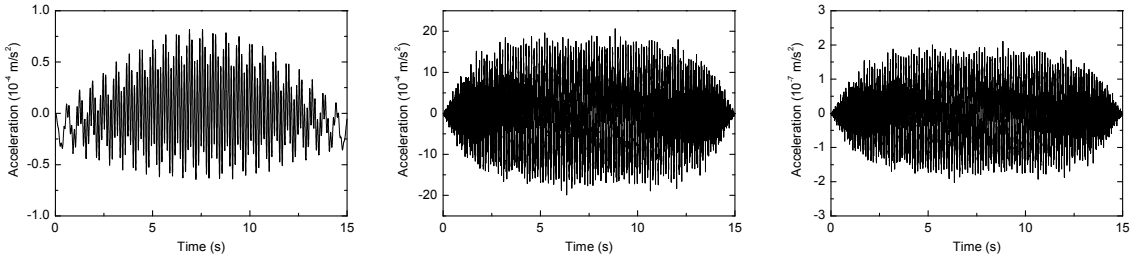

(a) a_1 (b) a_{c1} (c) $\bar{a}$

Figure 2. Acceleration histories under smooth surface condition

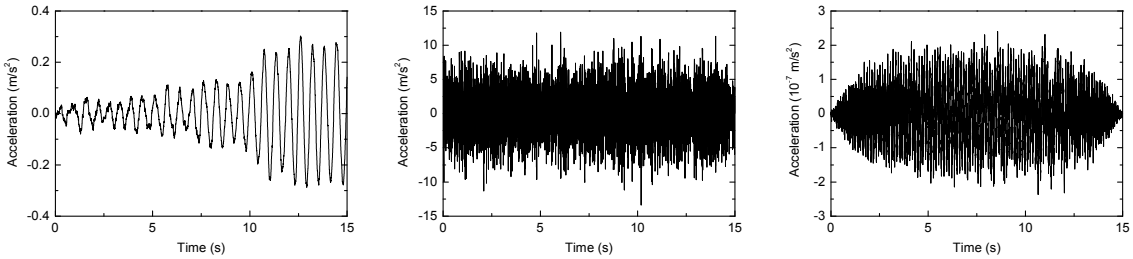

(a) a_1 (b) a_{c1} (c) $\bar{a}$

Figure 3. Acceleration histories under Class C (average quality) surface roughness condition

The vehicle acceleration a_1, contact point acceleration a_{c1} and NCPA $\bar{a}$ under smooth surface condition are presented in Figure 2, and those under Class C (average quality) surface roughness condition are shown in Figure 3. One can find that the surface roughness has a significant

influence on the value of vehicle acceleration and contact point acceleration, but NCPA are almost identical for both smooth and rough surface conditions.

The vehicle acceleration and contact point acceleration both contain bridge information and it is feasible to extract the bridge frequencies from them, which can be viewed from their spectra as shown in Figures 4(a) and 4(b). However, they are both very sensitive to the contamination of surface roughness. Even when very mild surface roughness is introduced, the bridge information is masked by the noise caused by the surface roughness and cannot be identified, as observed from Figure 5(a) and 5(b). It is also found that under smooth surface condition, the first three bridge frequencies can be identified clearly from the contact point acceleration, while even the second frequencies can hardly be identified from the vehicle acceleration. This shows the superiority of using contact point acceleration to extract bridge information over vehicle acceleration. However, the contact point acceleration is more prone to the contamination of surface roughness.

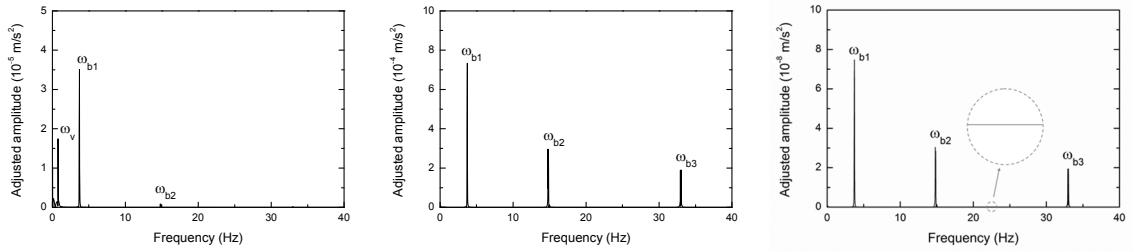

(a) Spectrum of a_1 (b) Spectrum of a_{c1} (c) Spectrum of $\bar{a}$

Figure 4. Frequency spectra of acceleration histories with smooth bridge surface

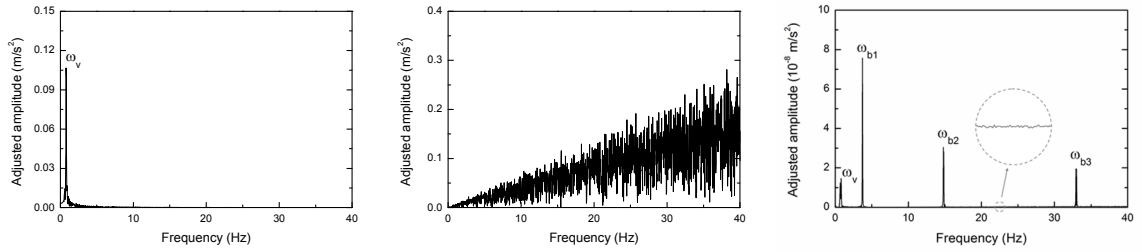

(a) Spectrum of a_1 (b) Spectrum of a_{c1} (c) Spectrum of $\bar{a}$

Figure 5. Frequency spectra of acceleration histories with Class C bridge surface roughness

It can be observed that the bridge frequencies can be clearly identified from NCPA. In contrast with the vehicle acceleration and contact point acceleration, NCPA is very much immune to the influence of surface roughness. Comparing Figure 4(c) with Figure 5(c), one can find that the influence of surface roughness leads to a peak at the vehicle frequency ω_v and some noise with small magnitude.

The mode shapes can be constructed from NCPA following the steps described in Section 3.1. The modal assurance criteria (MAC) is adopted to evaluate the performance of the detection results, as defined by Eq. (18), where φ_e is the extracted mode shape and φ_t is the theoretical mode shape. The detection outcome is presented in Table 1.

$$\text{MAC} = \frac{\varphi_e^T \varphi_t}{|\varphi_e||\varphi_t|} \tag{18}$$

Damage detection based on the mode shapes obtained is therefore feasible. Two damage cases with single and double damage elements are presented in Figure 6, where the damage is taken as 30% reduction of element stiffness.

Table 1. MACs of the mode shapes identified from NCPA

Order	Surface roughness class					
	Smooth	A (very good)	B (good)	C (average)	D (poor)	E (very poor)
1st	0.9999	0.9999	0.9997	0.9993	0.9988	0.9961
2nd	0.9999	0.9999	0.9999	0.9995	0.9971	0.9929
3rd	0.9999	0.9998	0.9991	0.9986	0.9914	0.9878

Note: The MACs presented are average values of those of the ten cases with different randomly generated surface roughness profiles in that class except for the column of smooth surface.

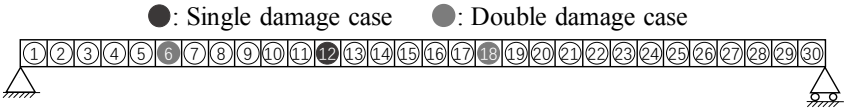

Figure 6. Finite element mesh of bridge and damage locations

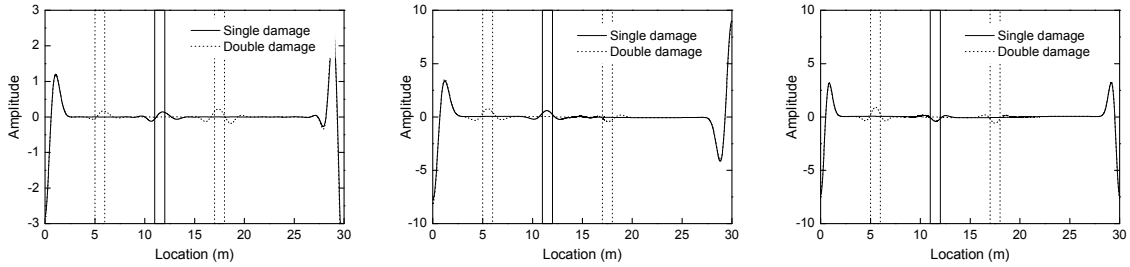

(a) 1st (b) 2nd (c) 3rd

Figure 7. Wavelet coefficients of mode shapes for single and double damage cases

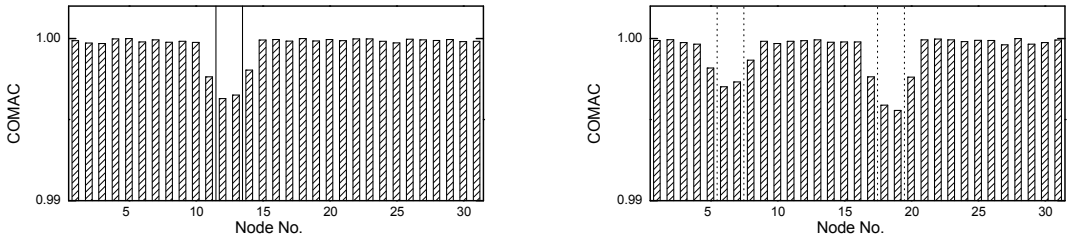

(a) Single damage case (b) Double damage case

Figure 8. Damage detection results of COMAC

Figure 7 show the wavelet transform coefficients of the mode shapes of the two damage cases, where damaged areas are marked with vertical solid lines for single damage case and vertical dot lines for double damage case. The damage can be located at the place where the wavelet coefficient has a sudden change or maximum. False alarm may occur near the two end supports where the rotational stiffness is close to zero, and similar phenomenon has been observed by other researchers such as Hester and González (2012). Figure 8 shows the COMAC calculated

using the first three mode shapes. Elements related to nodes with low COMAC is also a sign of damage. A combination of wavelet transform and COMAC could give clearer information about the damage location. These results are under Class C surface roughness condition, but similar results can also be found for other classes of roughness.

5 CONCLUSIONS

A method to identify the bridge modal parameters and locate possible damage using the response of a passing vehicle is proposed and verified numerically. The superiority of contact point response over the normally adopted vehicle chassis response is that the higher modes are more identifiable and only the bridge related frequencies are involved. Then the application of NCPA obtained by the double-pass method to mitigate the influence of surface roughness is investigated. It is found that the bridge frequencies and mode shapes can be extracted from NCPA in the presence of surface roughness, where other quantities such as the vehicle acceleration and contact point acceleration are ineffective. Finally, the damage locations can be identified from the mode shapes obtained using the wavelet transform and COMAC.

There are, however, still issues to resolve for application of the proposed method to a real bridge, e.g. the effects of daily temperature and possible change of boundary condition on the modal parameters and consequent damage detection. Further work is necessary to account for such effects, e.g. the method by Li et al (2010), especially for those bridges that are sensitive to such effects.

REFERENCES

Bu, J. Q., S. S. Law, and X. Q. Zhu, 2006, Innovative bridge condition assessment from dynamic response of a passing vehicle. *Journal of Engineering Mechanics*, 132(12), 1372-1379.

Cheng, Y. S., F. T. K. Au, Y. K. Cheung, and D. Y. Zheng, 1999. On the separation between moving vehicles and bridge. *Journal of Sound and Vibration*, 222(5), 781-801.

Hester, D., and A. González, 2012, A wavelet-based damage detection algorithm based on bridge acceleration response to a vehicle. *Mechanical Systems and Signal Processing*, 28, 145-166.

International Organization for Standardization (ISO), 2016, Mechanical vibration-road surface profiles-reporting of measured data.

Li, H., S. Li, J. Ou, and H. Li, 2010. Modal identification of bridges under varying environmental conditions: temperature and wind effects, 2010. *Structural Control and Health Monitoring*, 17(5), 495-512.

Li, Z. H., and F. T. K. Au, 2014, Damage detection of a continuous bridge from response of a moving vehicle. *Shock and Vibration*.

Qi, Z. Q., and F. T. K. Au., 2017, Identifying mode shapes of girder bridges using dynamic responses extracted from a moving vehicle under impact excitation. *International Journal of Structural Stability and Dynamics*, 17(08), 1750081.

Yang, Y. B., C. W. Lin, and J. D. Yau, 2004, Extracting bridge frequencies from the dynamic response of a passing vehicle. *Journal of Sound and Vibration*, 272 471–493.

Yang, Y. B., Y. C. Li, and K. C. Chang, 2014, Constructing the mode shapes of a bridge from a passing vehicle: A theoretical study. *Smart Structures and Systems*, 13(5) 797–819.

Zhan, Y., and F. T. K. Au, 2019, Bridge surface roughness identification based on vehicle-bridge interaction. *International Journal of Structural Stability and Dynamics*, doi: 10.1142/S021945541950069X.